British Journal of Pharmacology

British Journal of Pharmacology (2016) **173** 1314–1328 1314

RESEARCH PAPER

The novel nonapeptide acein targets angiotensin converting enzyme in the brain and induces dopamine release

Correspondence Jean Martinez, Institut des Biomolécules Max Mousseron (IBMM) UMR 5247, Département des Acides Aminés, Peptides et Protéines, Faculté de Pharmacie, Université de Montpellier, 14 Av. C. Flahault, Montpellier, 34095, France. E-mail: martinez@univ-montp1.fr

Received 13 June 2015; **Revised** 20 December 2016; **Accepted** 8 January 2016;

Jérémie Neasta[1], Charlène Valmalle[1], Anne-Claire Coyne[2†], Eric Carnazzi[1], Gilles Subra[1], Jean-Claude Galleyrand[1], Didier Gagne[1], Céline M'Kadmi[1], Nicole Bernad[1], Gilbert Bergé[1], Sonia Cantel[1], Philippe Marin[3], Jacky Marie[1], Jean-Louis Banères[1], Marie-Lou Kemel[4‡], Valérie Daugé[2†], Karine Puget[1‡] and Jean Martinez[1*]

[1]*Faculté de Pharmacie, Institut des Biomolécules Max Mousseron (IBMM) UMR 5247, Université de Montpellier, CNRS, ENSCM, Montpellier, France,* [2]*INSERM UMR 952, Physiopathologie des Maladies du Système Nerveux Central, Paris, France,* [3]*Institut de Génomique Fonctionnelle, UMR5203, INSERM U661, Rue de la Cardonille, Université de Montpellier, Montpellier, France, and* [4]*CIRB, Collège de France, 11, Place Marcelin Berthelot, Paris, France*

[*]Present address: Hôpital Armand Trousseau, RaDiCo-Inserm U933, Bâtiment Lemariey, 26 Avenue du Dr. Netter, 75012 Paris, France
[†]Present address: INRA, UMR 1319, MICALIS, F-78350 Jouy-en-Josas, France
[‡]Present address: GENEPEP SA, Les Côteaux Saint Roch, 12 rue du Fer à Cheval, 34430 St Jean de Védas, France
[**]Present address: Aviesan, Institut Thématique Multi-Organismes Neurosciences, Sciences Cognitives, Neurologie, Psychiatrie, 8 rue de la Croix Jarry, 75013 PARIS, France

BACKGROUND AND PURPOSE

Using an in-house bioinformatics programme, we identified and synthesized a novel nonapeptide, H-Pro-Pro-Thr-Thr-Thr-Lys-Phe-Ala-Ala-OH. Here, we have studied its biological activity, *in vitro* and *in vivo*, and have identified its target in the brain.

EXPERIMENTAL APPROACH

The affinity of the peptide was characterized using purified whole brain and striatal membranes from guinea pigs and rats . Its effect on behaviour in rats following intra-striatal injection of the peptide was investigated. A photoaffinity UV cross-linking approach combined with subsequent affinity purification of the ligand covalently bound to its receptor allowed identification of its target.

KEY RESULTS

The peptide bound with high affinity to a single class of binding sites, specifically localized in the striatum and substantia nigra of brains from guinea pigs and rats. When injected within the striatum of rats, the peptide stimulated *in vitro* and *in vivo* dopamine release and induced dopamine-like motor effects. We purified the target of the peptide, a ~151 kDa protein that was identified by MS/MS as angiotensin converting enzyme (ACE I). Therefore, we decided to name the peptide acein.

CONCLUSION AND IMPLICATIONS

The synthetic nonapeptide acein interacted with high affinity with brain membrane-bound ACE. This interaction occurs at a different site from the active site involved in the well-known peptidase activity, without modifying the peptidase activity. Acein, *in vitro* and *in vivo,* significantly increased stimulated release of dopamine from the brain. These results suggest a more important role for brain ACE than initially suspected.

Abbreviations

Abz, o-aminobenzoic acid; AD, Alzheimer's disease; Bpa, p-benzoyl-phenylalanine; DA, dopamine; Dnp, 2,4-dinitrophenyl; PD, Parkinson's Disease; RAS, renin-angiotensin system

DOI:10.1111/bph.13424
© 2016 The British Pharmacological Society

Tables of Links

TARGETS
Enzymes[a]
ACE1, angiotensin converting enzyme
GPCRs[b]
AT_1 receptor
D_1 receptor
D_2 receptor

LIGANDS
Captopril
Dopamine
Lisinopril
Sulpiride
SCH 23390

These Tables list key protein targets and ligands in this article, which are hyperlinked to corresponding entries in http://www.guidetopharmacology.org, the common portal for data from the IUPHAR/BPS Guide to PHARMACOLOGY (Pawson *et al.*, 2014) and are permanently archived in the Concise Guide to PHARMACOLOGY 2015/16 ([a,b]Alexander *et al.*, 2015a,b).

Introduction

The search for new biological targets that may lead to drug discovery is an important concern for research, in both academia and pharmaceutical companies (Shenone *et al.*, 2013). The challenge is to identify new molecules that potently and selectively interact with protein targets to modulate their biological activity. Peptides and their protein receptors, which play critical roles in normal and pathological physiology, are among the candidates. The search for new peptides and proteins using bioinformatics has been quite popular in recent years (Hinuma *et al.*, 2000; Amare *et al.*, 2006; Hummon *et al.*, 2006; Mirabeau *et al.*, 2007). Using an 'in-house' bioinformatics programme, we searched in EST databases for putative natural amidated peptides, an important family of peptide hormones exhibiting remarkable biological activities. Briefly, the programme (i) translates the cDNA sequences into proteins, (ii) selects proteins containing the characteristics of an amidated peptide precursor, (iii) mimics the intracellular enzyme systems on these precursors, (iv) provides peptide sequences of amidated peptides and (v) takes away all already known amidated peptides. More than 4500 sequences of unknown amidated peptides having less than 30 amino acid residues were identified (Martinez and Goze, 1999; Camara *et al.*, 2000), and more than 3000 were synthesized, along with their ^{125}I-labelled parent peptides. They were tested for their ability to bind to guinea pig whole brain membranes, known to contain most of the neuropeptide receptors. From the parent amidated peptide, we have identified a synthetic nonapeptide of sequence H-Pro-Pro-Thr-Thr-Thr-Lys-Phe-Ala-Ala-OH (JMV3041), which was named acein and was studied for its biological *in vitro* and *in vivo* activity in the CNS. Additionally, its protein target was characterized.

Methods

Animals

All animal care and experimental procedures complied with the NIH Guidelines for the Care and Use of Laboratory Animals and were approved by the local Ethical committee. Animal studies are reported in compliance with the ARRIVE guidelines (Kilkenny *et al.*, 2010; McGrath & Lilley, 2015).

Male guinea pigs (Charles River, Saint-Aubin les Elbeuf, France) weighing 200–300 g and male Sprague–Dawley rats (Charles River, Saint-Aubin les Elbeuf, France) weighing 200-225 g at the time of surgery and 300-350 g at the time of the behavioural experiments were used. Animals were housed in groups of four in a well-ventilated, temperature-controlled (22 ± 1°C) and humidity-controlled (50 ± 5%) environment. The animal room was maintained on a 12 h light–dark cycle (lights on at 7.30 AM). They had food and water *ad libitum*. Whenever possible, cell lines were used to obtain the results, instead of animals. When animals were used, they were randomly chosen and the group sizes are indicated for each set of experiments. The minimum number of animals to obtain statistically significant results was used and did not include replicates.

Peptide synthesis

All peptides were synthesized using classical Fmoc solid-phase peptide synthesis (Chan and White, 2000) and characterized by HPLC and LC/MS. HPLC analyses were carried out on a Waters 996 system using a Merck Chromolith Speed Rod C-18, 4.6 × 50 mm reversed-phase column (Merck Darmstadt, Germany). A flow rate of 5 mL·min^{-1} and a gradient of 0–100% B over 3 min was used (eluent-A: water/0.1% TFA, eluent-B: acetonitrile/0.1% TFA). Compounds were detected at 214 nm. The LC/MS system consisted of a Waters Alliance 2690 HPLC coupled to a Waters Micromass Quattro Micro spectrometer (electrospray ionisation mode). A Merck Chromolith Speed Rod C-18, 4.6 × 25 mm reversed-phase column was used. A flow rate of 1.2 mL·min^{-1} and a gradient of 0–100% B over 4 min were used (eluent-A: water/0.1% HCO_2H, eluent-B: acetonitrile/0.1% HCO_2H).

Radioiodination of ligands

[^{125}I]-Radiolabelled ligands were synthesised using the chloramine T method (Greenwood *et al.*, 1963) and purified by HPLC as previously described (Leyris *et al.*, 2011). Briefly, acein and acein analogues were dissolved in 0.5 M PBS pH 7.5 at a 10^{-3}M concentration. 10μL (37 MBq, 1mCi) of [^{125}I] NaI (PerkinElmer) was added to 10 μL of the peptide solution.

The reaction was initiated by adding 10 μL of a freshly prepared chloramine T solution (1mg·mL^{-1} in 0.5 M PBS pH 7.5). After intermittent stirring at room temperature for 2 min, the reaction was stopped by addition of 400 μL of a freshly prepared $Na_2S_2O_5$ solution (2 mg·mL^{-1} in 0.5M PBS pH 7.5). The mono-iodinated acein and acein analogues were purified by HPLC using a C18 column (elution with 0.1% trifluoroacetic acid and 10 % acetonitrile for 5 min, followed by a linear acetonitrile gradient of 10 to 40% developed over 30 min at a flow rate of 1.0 mL·min^{-1}.

Competition and binding experiments

Competition and binding experiments were performed in binding buffer (100 mM Na_2HPO_4-KH_2PO_4 pH 7.4, 4 mM $MgCl_2$, 0.1% BSA) following the protocol already described (Mousseaux *et al.*, 2006) using: (i) guinea pig whole brain membranes; (ii) guinea pig striatum membranes; (iii) CHO cell membranes prepared from CHO cells overexpressing human ACE (CHO-ACE cells) as described by Wei *et al.* (1991).

Competition binding experiments were performed using a final concentration of 0.2-0.5 nM of [^{125}I]-Tyr-acein ([^{125}I]-JMV3042), in the presence of increasing concentrations of a non-labelled ligand. Assays were initiated by addition of membranes (15 μg - 40 μg proteins per assay) and incubated for 40 min before filtration on Whatman GF/C filter.

Saturation binding experiments were performed using [^{125}I]-Tyr-acein over a final concentration range from 10^{-11} to 10^{-5} M. Non-specific binding was determined by adding a final concentration of 10 μM non-labelled H-Tyr-acein (JMV3042). Radioactivity in the membrane pellets was counted using a γ counter. All K_i constants were determined using GraphPad PRISM v6 software (GraphPad Software Inc., San Diego, USA).

Competition binding experiments on crude plasma membranes of HEK293T cells expressing the angiotensin AT_1 receptor are described in the Supporting Information section.

Photoaffinity labelling of the acein binding sites

Guinea pig striatal membranes were incubated for 20 min at 30°C with the photoactivatable and radio-labelled probe [^{125}I]-Tyr-Bpa-Pro-Pro-Thr-Thr-Thr-Lys-Phe-Ala-Ala-OH ([^{125}I]-Tyr-Bpa-acein) (1.5 nM), in binding buffer containing protease inhibitors (100 mM Na_2HPO_4-KH_2PO_4 pH 7.4, 4 mM $MgCl_2$, 0.1 mM PMSF, 0.02% soybean trypsin inhibitor and 0.1% BSA), then irradiated on ice with UV light (365 nm – 100 W) for 60 min. Photolabelling was stopped by centrifugation at 20 000 × *g* for 5 min at 4°C. The pellet was washed with the binding buffer containing 2% BSA, and the suspension was centrifuged for 5 min at 4°C at 20 000 × *g*. This washing step was repeated four times with a decreasing concentration of BSA in the washing buffer. Non-specific labelling was determined in the presence of 10 μM H-Tyr-Bpa-acein. The final pellet was suspended in SDS-PAGE buffer (62.5 mM Tris/HCl pH 6.8, 2% SDS, 10% glycerol, 5% 2-mercaptoethanol and 0.001% bromophenol blue). Samples were analysed by electrophoresis on 7% SDS-polyacrylamide gels and then dried and exposed to Kodak BioMax MS films with a Kodak BioMax TranScreen HE intensifying screen at −80°C.

Localization of acein binding sites in the rat brain

Fresh frozen (−20°C) tissue sections (16 μm thick) were dried under an air flow. They were first incubated for 10 min at 20°C in 50 mM Tris/HCl buffer with 0.5 mM EDTA, 3 mM $MgCl_2$ and 0.1% BSA. Sections were then incubated for 90 min at 20°C in 10 nM [^{125}I]-Tyr-acein ([^{125}I]-JMV3042) (specific activity = 2200 Ci·mmol^{-1}) in 120 mM Tris/HCl buffer containing 0.1% BSA. Non-specific binding was determined in the presence of 10 μM unlabelled peptide. Sections were then washed three times for 10 min at 4°C in 50 mM Tris/HCl buffer and finally quickly rinsed in ice-cold distilled water and air-dried. All sections were exposed to Kodak Biomax X-ray films at 4°C for 15 days. The films were developed in Kodak D-19 for 3 min at 20°C.

Enzymatic deglycosylation of the protein binding sites

The presence of N-carbohydrate side chains was determined by deglycosylation analysis of the binding sites cross-linked with [^{125}I]-Tyr-Bpa-acein using the Enzymatic In-Solution N-Deglycosylation Kit (GlycoProfile II) from Sigma.

Rotational behaviour

Stereotaxic implantations. Rats were anaesthetized with chloral hydrate (400 mg·kg^{-1},i.p.) and stereotaxically implanted with a unilateral 25-gauge stainless steel cannula guide, 1.5 mm above the right dorsal striatum. The coordinates, taken from the atlas of Paxinos and Watson (Paxinos and Watson, 2007), were: + 0.5 mm anterior, 3 mm lateral to the bregma and - 4.1 mm under the skull surface. The tip of the injection needle reached - 5.6 mm under the skull. Bilateral stainless steel cannula guides were implanted 0.5 mm above the sensorimotor territory of the striatum, defined by its specific cortical afferents (McGeorge and Faull, 1989; Berendse *et al.*, 1992), to test subsequent rotations. The coordinates were + 1.2 mm anterior, ± 4.25 mm lateral to the bregma. The cannula guide reached - 2.5 mm under the skull and the tip of the injection needle reached - 3 mm under the skull. Animals were used for experiments after a recovery period of 7 days.

Microinfusion procedure. Drugs and control solutions (0.9% NaCl) were injected unilaterally through the cannula guide as previously described (Sebret *et al.*, 1999). In the striatum, a volume of 5 μL over 2 min 20 sec was administered using a Precinorm pump (Infors, Bottminger, Switzerland) through a 30.5-gauge stainless needle attached to a 10 μL microsyringe (Hamilton) by polyethylene tubing. The stainless steel needle was 1.5 mm longer than the cannula guide and was left *in situ* for 60 s to allow diffusion of the drug. In the experiments carried out in the sensorimotor territory of the striatum, the stainless steel needle was 0.5 mm longer than the cannula guide and was left *in situ* for 60 s to allow diffusion of the drug. Drugs were injected in a volume of 0.5 μL over 1 min 32 s. The number of complete ipsilateral and contralateral rat rotations was counted for 8 min, starting 2 min after injection (Mendre *et al.*, 1988) (Supporting Information).

Pharmacological treatments. Acein (JMV3041), the selective D_1 receptor antagonist SCH23390 and the selective D_2 receptor antagonist sulpiride, were dissolved in saline 0.9%. SCH23390 (0.5 mL, 25 $\mu g \cdot kg^{-1}$ i.p.) was injected 30 min before JMV3041 intracerebral injection. Sulpiride (0.5 mL, 50 $mg \cdot kg^{-1}$ i.p.) was injected 2 h before acein intracerebral injection. The doses of dopamine receptor antagonists were chosen in agreement with previous reports (Mazurski and Beninger, 1991; Ladurelle *et al.*, 1997). Control animals were injected either in the striatum (5 µL) or in the sensorimotor territory (0.5 µL) with saline 0.9% and i.p. with saline 0.9% for animal treated with dopamine receptor antagonists.

Histological control. After completion of all microinjection experiments, animals were killed with an overdose of pentobarbital (100 $mg \cdot kg^{-1}$ i.p.), brains were removed and frozen in isopentane. Coronal sections were taken at the level of striatum with a cryostat (Leica, Nussloch, Germany). Sections were mounted on gelatin-coated slides and stained with cresyl violet. The position of the cannula was estimated according to the atlas of Paxinos and Watson (Paxinos and Watson, 2007).

Stimulation of striatal dopamine release by acein

In vitro NMDA-evoked release of [^{3}H]-dopamine in the sensorimotor territory of the dorsal striatum. Microsuperfusion was performed as previously described (Krebs *et al.*, 2002; Gras *et al.*, 2008). Brains were rapidly removed and chilled in a 4°C artificial cerebrospinal fluid (CSF in mM: NaCl, 126.5; $NaHCO_3$, 27.5; KCl, 2.4; $MgCl_2$, 0.83; KH_2PO_4, 0.5; $CaCl_2$, 1.1; Na_2SO_4, 0.5; glucose, 11.8). In each hemisphere, sagittal slices (1.2-1.5 mm) were cut with a vibratome at the appropriate laterality ($4 < \text{lateral} < 5$) in the sensorimotor territory, according to the atlas of Paxinos and Watson (Paxinos and Watson, 2007). Slices were then placed into a superfusion chamber containing CSF maintained at 34°C, saturated with O_2/CO_2 (95/5, v/v) and continuously renewed (750 $\mu L \cdot min^{-1}$). Microsuperfusion devices were vertically placed onto each selected area of the slices using micromanipulators and a dissecting microscope. Oxygenated CSF was continuously delivered through each superfusion device. This procedure allowed the superfusion of a limited volume of tissue (~ 0.2 mm^3) surrounding the inner tube of the microsuperfusion device.

The release of [^{3}H]-dopamine consisted of a labelling period (10 min, 30 $\mu L \cdot min^{-1}$) with CSF containing [^{3}H]-dopamine (1.78 $TBq \cdot mmol^{-1}$, 0.05 µM; Perkin Elmer) and reboxetine (2 µM) to prevent [^{3}H]-dopamine uptake into other monoaminergic neurons. Tissues were then washed (40 min) with non-labelled, reboxetine-containing CSF (60 $\mu L \cdot min^{-1}$). As the NMDA-evoked response only occurs in the absence of magnesium, tissues were washed with magnesium-free CSF-NMDA (1 mM + 10 µM D-serine) alone or with acein (1 and 10 nM) for 2 min, 50 min after the beginning of the washing period. [^{3}H]-dopamine release was measured for 30 min under constant delivery of the medium used during the washing period. Superfusates were collected in 5-min serial fractions and NMDA (1 mM) + D-serine (10 µM), were applied for 2 min in the fourth fractions. [^{3}H]-dopamine was counted in 200 µL aliquots of each fraction, using SuperMix liquid scintillation cocktail and a MicroBeta Trilux counter (Perkin Elmer). At the end of the superfusion, superfused tissues punched out from slices were dissolved in 200 µL 0.1 N HCl, 0.1% Triton X-100 to determine the total radioactivity contained in tissues at the end of the release period. The amount of [^{3}H]-dopamine release was expressed as a ratio of the total radioactivity calculated at the time of the collected fraction. Spontaneous release of [^{3}H]-dopamine was estimated during the two fractions preceding NMDA/D-serine application and [^{3}H]-dopamine released in each fraction was finally expressed as a percentage of the average spontaneous release. Statistical analyses were performed using SigmaStat 3,1 (Systat Software, San Jose, CA USA). In all cases, the release of [^{3}H]-dopamine during the NMDA-evoked response was determined after subtracting the corresponding spontaneous release estimated at the same time in slices not exposed to NMDA.

In vivo effect on the monoaminergic system in the striatum, using a brain dialysis procedure. The microdialysis probes used in the present investigation were of a vertical, concentric design and incorporated a dialysis membrane with an active length of 2 mm, as well as an injection cannula independent from the membrane (Microbiotech, Stockholm, Sweden), with a molecular size cut-off of 6 kDa. They were connected to a perfusion system previously described (Ladurelle *et al.*, 1995). Seven days before microdialysis experiments, rats were anaesthetized with chloral hydrate (400 $mg \cdot kg^{-1}$ i.p.) and stereotaxically implanted with a microdialysis probe guide cannula unilaterally inserted to a position 2 mm above the sensorimotor territory of the striatum, at the following coordinates: anteroposterior, + 1.2 mm, and lateral, + 3.5 mm from bregma and dorsoventral, - 3 mm, from skull surface (Paxinos and Watson, 2007). The guide was secured in place using skull screws and fast-curing dental cement. The evening before microdialysis experiments, the probe was inserted into the unilaterally implanted guide cannula and the rats were put into individual black boxes (40 × 40 × 40 cm) with free access to food and water to habituate them to this new environment and to the microdialysis system. Microdialysis probes were continuously perfused with a CSF (in mM: NaCl 140, KCl 4, $CaCl_2$ 1.2, $MgCl_2$ 1.4, NaH_2PO_4 0.1, Na_2HPO_4 1.9, pH = 7.4) at a rate of 2 µl·min by means of a Precinorm pump. After 2 h equilibration period of perfusion, dialysate samples were collected every 20 min. The baseline was established by four consecutive samples. Using a Precinorm pump, 5 fmol acein were then injected directly into the striatum through the injection cannula of the microdialysis probe attached to a 10 µL microsyringe (Hamilton) by polyethylene tubing, in a volume of 0.5 µL over 1 min 32 s. Dialysate samples were collected in vials and immediately stored at - 80°C until they were analysed by HPLC. They were injected into a 20 µL sample-loop of an HPLC apparatus and measurement of monoamines and metabolites was made by means of electrochemical detection (Decade, Antec) at a potential of 750 mV following reverse-phase liquid chromatography (HPLC), on a 10 cm column (Colochrom, 3.2 mm diameter, 3 µm C-18 packing). The mobile phase consisted of an acetate buffer containing 100 µM EDTA, 1 mM

octanesulfonic acid and 4 % (v/v) acetonitrile at pH 3.1, and was delivered at a flow rate of 1 ml·min^{-1}.

Histological control. After the completion of all microinjection and microdialysis experiments, the animals were overdosed with pentobarbital (100 mg·kg^{-1} i.p.), brains were removed and frozen in isopentane at - 20°C. Coronal sections were taken at the level of striatum with a cryostat. The sections were mounted on Superfrost^{R} Plus slides and stained with cresyl violet. The position of the cannula was estimated according to the atlas of Paxinos and Watson (Paxinos and Watson, 2007).

UV cross-linking of JMV5394 to guinea pig striatal membranes

Crude striatal membrane proteins (40 μg; 0.5 μg·μL^{-1} per assay) were incubated either with 50 nM JMV5394 for 40 min at 30°C in binding buffer containing 1 g·L^{-1} BSA, in polypropylene haemolysis tubes, with no other addition, or in the presence of an excess of H-Tyr-acein (JMV3042). The content of each tube was cooled on ice for 15 min and then transferred to a 12-well Nunclon plate and irradiated with UV light at 365 nm for 60 min at 4°C. Cross-linked membranes were then recovered by centrifugation (20 000 × *g*, 10 min, 4°C), and stored at − 80°C before subsequent analysis.

UV cross-linking of JMV5394 to rabbit lung ACE

Purified rabbit lung ACE (4 μg) was incubated either with 50 nM of JMV5394 for 40 min at 30°C in binding buffer containing 1 g·L^{-1} of BSA, in polypropylene haemolysis tubes, with no other addition, or in the presence of an excess of H-Tyr-acein or of ghrelin (Kojima *et al.*, 1999). The content of each tube was cooled on ice for 15 min, transferred to a 24-well Nunclon plate and irradiated with UV light at 365 nm for 60 min at 4°C. Then, mixtures were collected and stored at − 20°C before subsequent analysis.

Western blot analysis

Proteins were resolved by SDS-PAGE, 10% acrylamide gels; transferred to nitrocellulose membrane; and blocked for 60 min with 5% (w/v) non-fat milk in Tris–HCl buffered saline containing 0.1% (v/v) Tween 20 (TBS-T). The ACE protein was detected with an anti-ACE antibody (incubated at 4°C, overnight) followed by incubation with goat anti-mouse HRP-conjugated antibody. Biotinylated proteins were detected with streptavidin overlay with a Vectastain Elite ABC system according to the provider's instruction. In both cases, after extensive washes with TBS-T, relevant proteins were detected and visualized by ECL advance (GE Healthcare, Little Chalfont, UK).

Pull down of the biotinylated ligand–receptor complex

Striatal membrane proteins (400 μg) were UV cross-linked to 50 nM of JMV5394 as described earlier, followed by sonication in 650 μL of pull-down buffer (20 mM Tris–HCl, 150 mM NaCl, 0.1% (w/v) SDS at pH 7.4, supplemented with protease inhibitors). After 60 min gentle stirring at room temperature, non-solubilized proteins were discarded by centrifugation at 16 000 × *g* for 10 min at 4°C, and the supernatant was incubated with 25 μL of streptavidin agarose resin for 90 min at room temperature. Agarose resin was discarded by centrifugation at 2500 × *g* for 1 min. The supernatant, which contained the JMV5394-receptor complex, was saved, and proteins were reduced for 30 min at 60°C with 10 mM DTT followed by incubation with 30 mM iodoacetamide for 60 min at room temperature, in the dark. The mixture was then adjusted to 900 μL with pull-down buffer and residual biotinylated proteins were pulled-down with 25 μL of streptavidin agarose resin for 90 min at room temperature. The agarose resin was extensively washed with 3 mL of 20 mM Tris–HCl, 500 mM NaCl, 0.1% (w/v) SDS, pH 7.4 and then with 2 mL of pull-down buffer. Pull-downed proteins were eluted at 95°C for 15 min in SDS-PAGE buffer (2% SDS, 200 mM DTT, 50 mM Tris–HCl, pH 6.8, 10% glycerol, 1 mM EDTA and 0.1% bromophenol blue) and resolved by 10% SDS-PAGE.

Silver staining

SDS-PAGE gels were stained with SilverQuest staining kit according to the provider's instructions.

Mass spectrometry analysis

Protein separation and trypsin digestion. Samples were separated by a 10% SDS PAGE after 15 min (97°C) denaturation. Silver colouration and enzymic in-gel digestion were performed according to the Shevchenko modified protocol (Wilm *et al.*, 1996). Briefly, digestion was performed overnight at 30°C, with shaking, with 800 ng trypsin (Gold, Promega) in 50 mM triethylammonium bicarbonate buffer. Tryptic fragments were extracted with 50% acetonitrile and 5% formic acid and dehydrated in a vacuum centrifuge.

Identification by nano LC–MS/MS. Generated peptides were solubilized in 6 μL of 0.1% formic acid and 2% acetonitrile and analysed online by nano-flow HPLC–nanoelectrospray ionization using a LTQ Orbitrap XL mass spectrometer (Thermo Fisher Scientific, Waltham, USA) coupled with an Ultimate 3000 HPLC (Thermo Fisher Scientific). Desalting and pre-concentration of samples were performed online on a Pepmap® precolumn (0.3 mm × 10 mm; Thermo Fisher Scientific). A gradient consisting of 0-40% B for 60 min, followed by 80% B/20% A for 15 min (A = 0.1% formic acid, 2% acetonitrile in water; B = 0.1% formic acid in acetonitrile) at 300 nL·min^{-1}, was used to elute peptides from the capillary (0.075 mm × 150 mm) reversed-phase column (Acclaim® PepMap100 C18; Thermo Fisher Scientific), fitted with an uncoated silica PicoTip Emitter (NewOjective, Woburn, MA, USA). Eluted peptides were electrosprayed online at a voltage of 2.20 kV into an LTQ Orbitrap XL mass spectrometer. Source parameters were adjusted as follows: ion spray voltage, 2.20 kV; capillary voltage, 43 V; and tube lens, 120 V. A cycle of one full-scan mass spectrum (400–2000 m/z) at a resolution of 60 000 (at 400 m/z), followed by five data-dependent MS/MS spectra, was repeated continuously throughout the nano LC

separation. Data were acquired using the Xcalibur software (v 2.0.7, Thermo Fisher Scientific).

All MS/MS spectra were recorded using normalized collision energy (35%, activation Q 0.25 and activation time 30 ms) with an isolation window of 3 m/z. For all full scan measurements with the Orbitrap detector, a lock mass ion from ambient air (m/z 445.120024) was used as an internal calibrant as described (Olsen *et al.*, 2005). All MS/MS spectra were searched against the *Cavia porcellus* entries (20 368 entries) of either Swiss-Prot or TrEMBL databases (release 2013_03; http://www.uniprot.org/) by using the Proteome Discoverer v1.4 software (Thermo Fisher Scientific) and the Mascot v2.4 algorithm (Matrix Science, http://www.matrixscience.com/) with trypsin enzyme specificity and one trypsin-missed cleavage. Carbamidomethyl was set as fixed cysteine modification. The search was also performed allowing the following variable modification: oxidation (M). The mass tolerances in MS and MS/MS were set to 5 ppm and 0.5 Da respectively. The instrument setting was specified as 'ESI-TRAP' for identification. Management and validation of MS data were performed using the Proteome Discoverer software (peptide identifications were accepted based on their false discovery rate (<5%).

Continuous fluorescent assay of ACE activity from purified rabbit lung ACE and CHO-ACE cell membranes

The enzymic activity of either CHO-ACE membranes (6 μg) or purified rabbit ACE was assayed by continuous fluorescent assay with 10 μM of the internally quenched fluorescent peptide Abz-FRK(Dnp)P-OH (Carmona *et al.*, 2006) as substrate and determined at 37°C in a buffer containing 90 mM Tris–HCl, 90 mM NaCl, 18 μM $ZnSO_4$ and pH 7.2, in a 96-well flat black plate. The hydrolysis of Abz-FRK(Dnp)P-OH into the dipeptide Abz-FR was monitored every 0.5 min for 30 min with the Tekan Infinite 200 PRO fluorimeter by measuring fluorescence at λex = 320 nm and λem = 420 nm. The slope, representing the relative activity of ACE, was calculated by linear regression from 5 to 30 min of the time course by Magellan data analysis software (Tekan). The assay was also performed in the presence of either captopril or lisinopril, two selective ACE inhibitors.

Data and statistical analysis

These studies complied with the recommendations on experimental design and analysis in pharmacology (Curtis *et al.*, 2015). Data of *in vitro* binding, saturation and enzyme experiments are at least from 3 to 5 separate experiments performed in duplicate and are expressed as means ± SEM unless otherwise stated. *In vitro* and *in vivo* data of striatal dopamine release are expressed as means ± SEM and values are from 9 separate experiments. Behavioural data are expressed as means ± SEM for each parameter in the diverse groups of treatment. The statistical analysis of these results consisted of a one-way (treatment) ANOVA and a Newman-Keuls or Tukey's test for multiple comparisons. A Dunnett test was used for comparison with control group. The 5% level ($P < 0.05$) for statistical significance was chosen *a priori*.

Materials

Amino acid derivatives, *p*-benzoyl-phenylalanine (Bpa), biotin and amino hexanoic acid were from IRIS-Biotech, Germany. Streptavidin agarose resin (#20361) was purchased from Pierce, anti-ACE antibody was purchased from Abcam Cambridge, MA, USA (# ab11734), purified ACE from rabbit lung (#A6778) and its fluorescent substrate *o*-aminobenzoic acid (Abz)-FRK[2,4-dinitrophenyl (Dnp)]P-OH (#A4980) were purchased from SIGMA ALDRICH, St Louis, MO, USA. Captopril and lisinopril were obtained from SIGMA-ALDRICH, St Louis, MO, USA. Vectastain Elite ABC system (#PK-6100) was from Vector Laboratories (Burlingame CA, USA). SilverQuest™ staining kit was purchased from Invitrogen (Cergy-Pontoise, France). CHO-ACE cells with no mycoplasma contamination were used to prepare membranes and were provided by P. Corvol and A. Michaud (Collège de France, Paris).

Results

Binding experiments to guinea pig brain membranes

Saturation experiments carried out with [^{125}I]-Tyr-acein, followed by non-linear regression analysis of saturation binding data, revealed that the peptide recognized a single class of binding sites in guinea pig whole brain membranes (correlation coefficient 0.93), with high affinity (K_d = 0.89 ± 0.25 nM) and a maximal number of binding sites (B_{max}) of 78.5 ± 5.0 fmol·mg^{-1} protein (Figure 1A). Binding was saturable and specific. In competition experiments, acein displaced [^{125}I]-Tyr-acein from whole brain guinea pig membranes with high affinity (K_i = 5 ± 1 nM) (Table 1). On whole brain guinea pig brain membranes, at 1 μM, neither cholecystokinin, neurotensin, substance P, Leu-enkephalin, Met-enkephalin, bombesin, nociceptin nor neurotransmitters, such as dopamine, 5-HT and GABA, were able to displace labelled acein from its binding sites (Table S1). Similarly, H-Tyr-acein (1 μM) did not displace labelled angiotensin II on HEK 293T cells expressing AT_1 receptors (n = 5).

Localization of peptide binding sites

Autoradiography with [^{125}I]-Tyr-acein revealed acein binding sites in both the substantia nigra and the striatum of rat (Figure 2). The sagittal section indicated the presence of an intense labelling in the choroid plexus and the fourth ventricle, with weaker labelling in the cerebellum (Figure 2A). The coronal section of the striatum exhibited a higher density of peptide binding sites in the sensorimotor, compared with the limbic striatum (Figure 2B). There was no labelling observed in the nucleus accumbens. Labelling in the substantia nigra (Figure 2C) was mainly in the substantia nigra pars reticulata.

Binding experiments with guinea pig striatal brain membranes

In accordance with autoradiography experiments, [^{125}I]-Tyr-acein bound to a single class of binding sites on guinea pig striatal membranes (correlation coefficient 0.89), with high affinity (K_d = 0.71 ± 0.26 nM), and a maximal number of binding sites of 830 ± 94 fmol·mg^{-1} protein (Figure 1B).

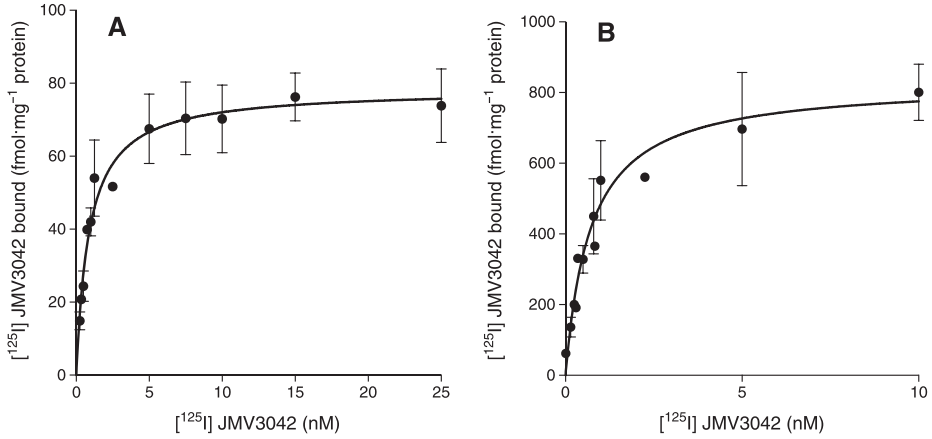


Figure 1

Characterisation of the binding properties of [^{125}I]-Tyr-acein ([^{125}I]-JMV3042) on guinea pig brain. Saturation experiments on guinea pig brain membranes were performed using [^{125}I]-JMV3042. (A) Total brain membranes and (B) striatal brain membranes. Non-specific binding was determined by adding a final concentration of 10 μM unlabelled acein. K_d and B_{max} values were determined by non-linear regression analysis of saturation binding data using GraphPad Prism v6 software. Reported values are means of three independent experiments performed in duplicate for total brain membranes and of five separate experiments performed in duplicate for striatal membranes.

Table 1

Structure and binding characteristics of acein and analogues on guinea pig brain and CHO-ACE membranes

Peptides	Names	Guinea pig K_i (nM)	CHO-ACE K_i (nM)
H-Pro-Pro-Thr-Thr-Thr-Lys-Phe-Ala-Ala-OH	JMV3041, acein	5 ± 1	14 ± 4
H-Tyr-Pro-Pro-Thr-Thr-Thr-Lys-Phe-Ala-Ala-OH	JMV3042, H-Tyr-acein	1 ± 0.6	13 ± 4
[^{125}I]-Tyr-Pro-Pro-Thr-Thr-Thr-Lys-Phe-Ala-Ala-OH	[^{125}I]-JMV3042		
[^{125}I]-Tyr-Bpa-Pro-Pro-Thr-Thr-Thr-Lys-Phe-Ala-Ala-OH	[^{125}I]-Tyr-Bpa-acein	3.7 ± 0.7	
Biot-Ahx-Tyr-Bpa-Pro-Pro-Thr-Thr-Thr-Lys-Phe-Ala-Ala-OH	JMV5394	5 ± 2	15 ± 5
H-Pro-Pro-Thr-Thr-Thr-Lys-Phe-Ala-(D)Ala-OH	JMV3068	>1000	>500

Competitive inhibition assays were performed on guinea pig whole brain membranes that were incubated with 0.2 nM [^{125}I]-Tyr-acein ([^{125}I]-JMV3042) for 40 min, in the presence of increasing concentrations of unlabelled acein or other unlabelled acein analogues. Values (±SEM) are representative of five separate experiments, each performed in duplicate. On CHO-ACE cell membranes, competition curves were obtained using 0.5 nM [^{125}I]-Tyr-acein, and data (±SEM) are representative of three separate experiments, each performed in duplicate.

Behavioural effects of acein

We investigated the behavioural effect of acein in rats, following single direct unilateral injection within the dorsal striatum. This well-known model indicates dopaminomimetic effects when rats are prompted to rotate in tight head to tail turns (Mendre *et al.*, 1988); Acein (5 and 50 fmol) injected in the right dorsal striatum induced a significant increase of contralateral rotations (reverse to the injection site) (n = 10) [($F_{(3,36)}$ = 2.164, P = 0.03], [P < 0.05 vs. control (saline 0.9%), Dunnett's test] (Figure 3A). No significant modification of rearing and ipsilateral rotation was observed.

To validate the involvement of dopamine, the effect of dopamine receptor antagonists was investigated. While neither of the D_1 or D_2 receptor antagonists used (25 μg·kg^{-1} of the D_1 receptor selective antagonist SCH23390 or 50 mg·kg^{-1} of the selective D_2 receptor antagonist sulpiride) modified the behaviour of control rats in the test, they decreased the contralateral rotations induced by 50 fmol acein (n = 9) [$F_{(5,46)}$ = 6.530, P = 0.0001], [P < 0.01 vs. control (saline 0.9%)] (Figure 3B).

Given the heterogeneous distribution of the peptide binding sites within the dorsal striatum, acein was injected in the sensorimotor territory. The total number of rotations was increased upon injection of acein (0.5 and 5 fmol) in this territory (n = 10) [$F_{(2,28)}$ = 15.611, P < 0.001], (P < 0.001 vs. control, Dunnett's test) (Figure S1).

Stimulation of in vitro and in vivo striatal dopamine release by acein

To provide direct evidence for an action of acein on the striatal dopaminergic transmission, we measured the dopamine release from rat striatal slices taken from the sensorimotor territory. [^{3}H]-dopamine release was monitored by both

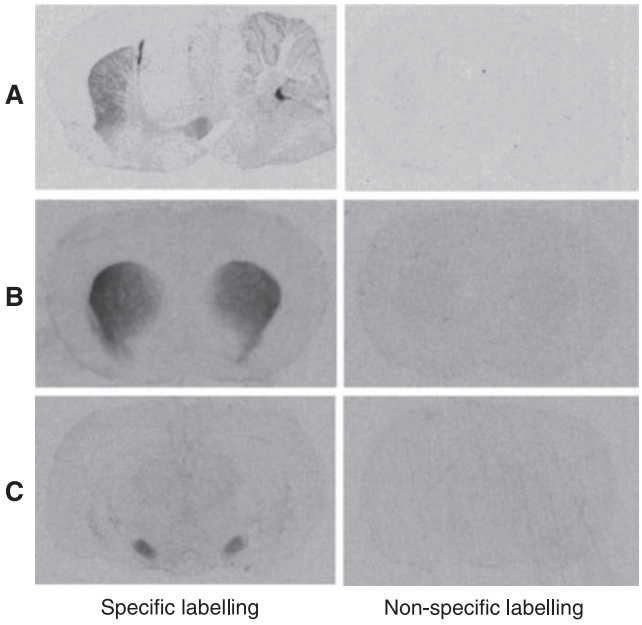


Figure 2

Binding sites labelling with [^{125}I]-Tyr-acein ([^{125}I]-JMV3042). (A) On sagittal rat brain sections, (B) on coronal rat brain sections at the striatum level and (C) on coronal rat brain sections at the substantia nigra level. Non-specific binding was determined using 10 μM acein. The figure is representative of five separate experiments.

microperfusion and scintillation counting. The [^{3}H]-dopamine release evoked by the glutamate receptor agonist NMDA (1mM), given together with D-serine (10μM), was almost double the basal release (increased by 97 ± 8%). Adding acein to the NMDA+D-serine stimulus increased dopamine release further to 240 ± 14% basal for 1 nM acein and to 281 ± 14% basal for 10 nM acein (n = 9; one-way ANOVA, $F_{(2,28)}$ = 12.6 (P < 0.001); Tukey's test, P < 0.05). This effect of acein was concentration-dependent (P<0.05) but dopamine release was not affected by treatment of the slices with acein alone.

To explore the ability of acein to regulate monoaminergic transmission in the striatum, dopamine release was quantified *in vivo*. Direct single injection of 5 fmol acein into the sensorimotor territory of dorsal striatum of rats rapidly produced a significant increase in dopamine efflux (Figure 4), inducing a maximal response 20 min after the injection, to about five-fold the pre-injection, basal, values (P < 0.001 vs. control, Dunnett's test). The efflux then decreased and returned to the basal value by 80 min after the injection. No effect was observed when saline was injected ($F_{(1,14)}$ = 4.68; P > 0.05).

Identification of the striatal protein target for acein

Cross-linking experiments on both whole and striatal guinea pig brain membranes using [^{125}I]-Tyr-Bpa-acein revealed a single protein band of about 160 kDa (Figure 5A and B), which was glycosylated (Figure 5C), with no indication of subunit composition linked through inter-disulphide bonds (Figure 5D).

To identify the striatal protein target of acein, we implemented a photoaffinity UV cross-linking approach combined with subsequent affinity purification of the covalent ligand–target complex. We synthesized a photoactivatable derivative of acein (JMV5394), containing a N-terminal aminohexanoic acid spacer flanked between the UV photoreactive Bpa and biotin, for further streptavidin affinity isolation of the biotinylated ligand–receptor complex. JMV5394 displayed high affinity for guinea pig brain membranes (K_i = 5 ± 2 nM) (Table 1). UV light irradiation of JMV5394 pre-incubated with guinea pig striatal membranes followed by resolution of proteins by SDS-PAGE and streptavidin overlay resulted in the detection of a single and specific band of approximately 160 kDa. When JMV5394 cross-linking was carried out in the presence of an excess of H-Tyr-acein, this band was absent (Figure S2A). These data indicated that UV cross-linking of JMV5394 to striatal membranes induced specific and irreversible formation of a biotinylated JMV5394-protein complex.

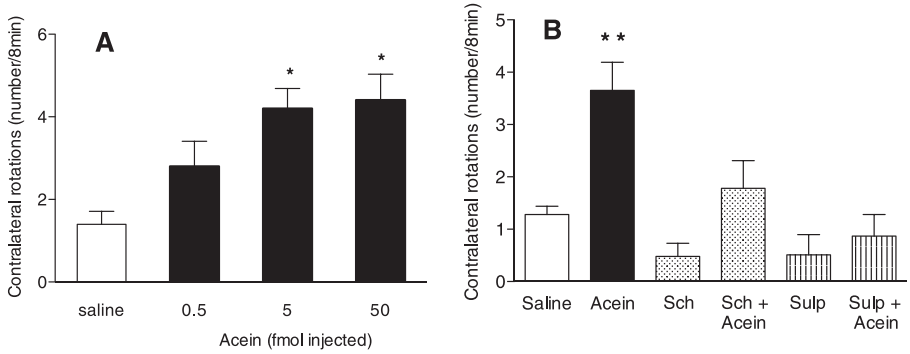


Figure 3

Acein-induced contralateral rotations in rat. (A) After unilateral injection of 0.5, 5 and 50 fmol acein (JMV3041) into the rat striatum. Data are expressed as means ±SEM (n = 10) [($F_{(3,36)}$ = 2.164, P = 0.03]. *P < 0.05 versus control (saline 0.9%), Dunnett's test. (B) Effect of selective D_1 or D_2 receptor antagonists. SCH23390 (Sch) (25 μg·kg^{-1}) was injected i.p. 30 min before acein (50 fmol). Sulpiride (Sulp) (50 mg·kg^{-1}) was injected i.p. 2 h before acein (50 fmol). Data are expressed as means ±SEM (n = 9) [$F_{(5,46)}$ = 6.530, P = 0.0001]. **P < 0.01 versus control (saline 0.9%) acein-treated rats, Newman test.

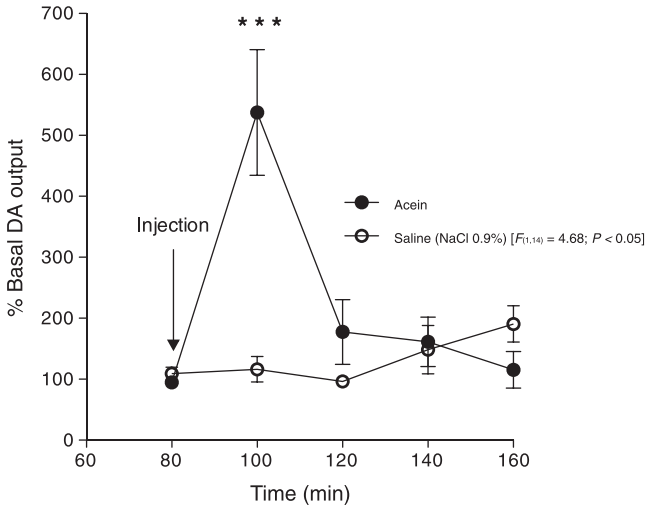


Figure 4

Acein-induced *in vivo* dopamine release in the rat striatum. Acein (JMV3041) (5 fmol) was injected into the sensorimotor territory of dorsal striatum. Dopamine (DA) efflux was measured for 80 min ($n = 9$ for each control and acein-treated groups). Results are expressed as the percentage of basal dopamine levels before any injection (means ± SEM: 1.88 ± 0.72 pg·μL^{-1}, control group saline 0.9% and 1.44 ± 0.51 pg·μL^{-1}, acein-treated group). These values correspond to the mean of the four samples collected every 20 min for the 80 min preceding the injection time. 100% = 1.76 pg·μL^{-1} (mean of the two basal values). ***$P < 0.001$ versus control, Dunnett's test.

The resulting biotinylated JMV5394–protein complex was pulled down using streptavidin agarose beads, followed by migration on SDS-PAGE and then detected by streptavidin overlay. A single biotinylated protein (~160 kDa) was detected. The same protein was also detected by silver-stained detection of pulled-down proteins (Figure S2B). To fully characterize protein contents in this band, it was extracted, digested and submitted to MS/MS analysis. Only peptide sequences corresponding to a ~151 kDa protein, named H0UWL7_CAVPO, from *C. porcellus*, were identified by MS/MS in the sample (Table S2 and Figure S2C). As H0UWL7_CAVPO was an uncharacterized protein, we blasted its amino acid sequence against UniProtKB/Swiss-Prot database and found that it shared a high degree of identity with rabbit, chimpanzee, human, rat and mouse ACE I (Bernstein *et al.*, 2013) (Figure S2D), thereby suggesting that this peptidase was a target for acein.

Validation of ACE as the protein target for acein

To confirm that ACE was the striatal protein target for acein, JMV5394 was first UV cross-linked to striatal membranes to induce formation of the biotinylated JMV5394–protein complex. Then, biotinylated proteins were pulled down with the streptavidin agarose resin, and the presence of ACE in pull-down complexes was examined after SDS-PAGE and Western blot analysis, using a monoclonal anti-ACE antibody. ACE was pulled down only in the absence of an acein excess, indicating the formation of an irreversible biotinylated JMV5394–ACE complex following UV light irradiation (Figure S3A). To further confirm that JMV5394 was bound to ACE, JMV5394 was pre-equilibrated with purified rabbit lung ACE, and after UV irradiation, formation of the biotinylated JMV5394–ACE complex was examined by streptavidin overlay. The JMV5394–rabbit ACE complex was indeed detected (Figure S3B). Cross-linking of JMV5394 to rabbit ACE was

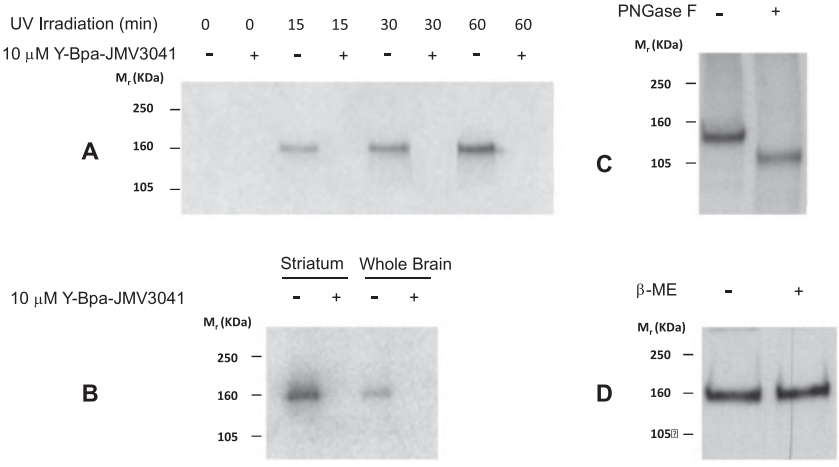


Figure 5

Photoaffinity labelling of binding sites. (A) Guinea pig striatal membranes were labelled with [^{125}I]-Tyr-Bpa-acein, analysed with SDS-PAGE and autoradiographed. UV light irradiation was performed for 0, 15, 30 and 60 min in the absence or in the presence of 10 μM H-Tyr-Bpa-acein. (B) Guinea pig striatal membranes and whole brain membranes were labelled with [^{125}I]-Tyr-Bpa-acein and incubated in the absence or presence of 10 μM H-Tyr-Bpa-acein. (C) Photoaffinity-labelled guinea pig striatal membranes were incubated 30 min in the absence or presence of 2.5 units peptide N-glycosidase F (PNGase F). (D) Comparison of non-reduced and reduced binding sites to determine the eventual multimeric association through disulphide bonds. Photoaffinity-labelled guinea pig striatal membranes were solubilized in Laemmli loading buffer in the absence or presence of 1 M β-mercaptoethanol (β-ME). The figure is representative of three experiments ($n = 3$).

specific and inhibited by an excess of H-Tyr-acein, but not by an excess of the unrelated peptide ghrelin (Kojima *et al.*, 1999). Taken together, these findings confirmed ACE as a striatal protein target for acein.

Binding experiments to CHO cells overexpressing human ACE (CHO-ACE cells)

For further validation, we performed binding experiments using CHO cells overexpressing human ACE (Wei *et al.*, 1991). Saturation experiments carried out with CHO-ACE cell membranes using [^{125}I]-Tyr-acein, followed by non-linear regression analysis of saturation binding data, revealed that this peptide recognized a single class of binding sites (correlation coefficient 0.97), with high affinity (K_d = 2.79 ± 1.53 nM) and a maximal number of binding sites of 10 200 ± 3100 fmol·mg^{-1} protein (Figure S4). In competition experiments, acein, H-Tyr-acein and JMV5394 were able to displace [^{125}I]-Tyr-acein with high affinity, on both guinea pig whole brain membranes and CHO-ACE cell membranes (Table 1, Figure S5). The acein analogue JMV3068, bearing a C-terminal D-Ala residue, had low affinity. Unexpectedly, captopril and lisinopril, two selective ACE inhibitors, displaced only about 50% [^{125}I]-Tyr-acein from its binding sites, with lower affinity (IC_{50} = 379 and 90 nM respectively) (Figure 6A), suggesting acein bound to ACE at sites different from that for the ACE inhibitors. Similar results were obtained on guinea pig striatal membranes in which captopril and lisinopril (IC_{50} > 1 μM and 145 nM respectively) were again unable to completely displace [^{125}I]-Tyr-acein from its binding sites (Figure 6B).

Effect of H-Tyr-acein on ACE enzymic activity

We further asked whether H-Tyr-acein might affect ACE enzymic activity either from CHO-ACE cell membranes (Figure 7A) or from purified rabbit lung ACE (Figure 7B), as measured by hydrolysis of the fluorescent ACE substrate Abz-FRK(Dnp)P-OH (Carmona *et al.*, 2006). No significant effect of H-Tyr-acein (up to 500 nM) on the peptidase activity was observed, either on CHO-ACE cell membranes or on purified rabbit lung ACE. As expected, captopril and lisinopril completely inhibited ACE peptidase activity in these preparations (Figures 7A and C).

Discussion

We have synthesised a nonapeptide, H-Pro-Pro-Thr-Thr-Thr-Lys-Phe-Ala-Ala-OH, which was named acein, which binds with high affinity and specificity to brain membranes of guinea pigs and rats. Acein binding sites were mainly localized in the dorsal striatum and substantia nigra areas of brain, where membrane-bound ACE is largely found (Zhuo *et al.*, 1998; Sonsalla *et al.*, 2013; Labandeira-Garcia *et al.*, 2014). In accordance with the known ACE localisation, there was a heterogeneous distribution of peptide binding sites within the striatum. Autoradiographic visualization of [^{125}I]-Tyr-acein and [^{3}H]-captopril binding sites (Strittmatter *et al.*, 1984) overlapped in the rat brain. We confirmed that acein was able to bind with high affinity to CHO-ACE cell membranes and that ACE was a target for acein.

We showed that acein at low doses exhibited a dopaminomimetic effect in rats. Interactions with the dopaminergic system were confirmed by using D_1 (SCH23390) and D_2 (sulpiride) dopamine receptor antagonists, which both prevented the behavioural effects induced by acein. In addition, we showed that acein stimulated, *in vitro*, the NMDA-evoked release of dopamine in rat brain slices and, *in vivo*, dopamine release in rats. These results suggest that the action of acein, associated with dopamine release, could be related to a peptidase-independent, unknown function of brain ACE, whose mechanism of action is still to be clarified.

ACE is a well-characterised, zinc-dependent, peptidyl-dipeptidase, widely studied for its role in the control of blood pressure by production of angiotensin II from angiotensin I and by degradation of bradykinin (Bernstein *et al.*, 2013). However, the enzyme is also involved in a large range of biological

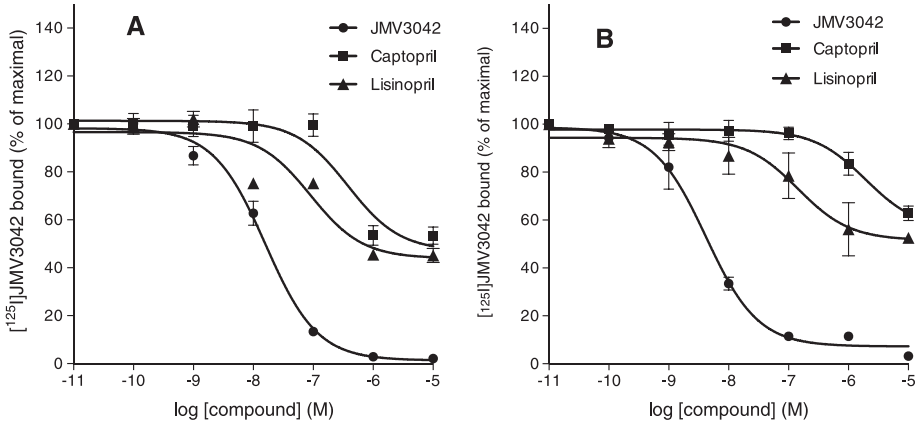


Figure 6

Binding properties of H-Tyr-acein (JMV3042) and ACE inhibitors to striatal and CHO-ACE cell membranes. Competition binding experiments used 0.5 nM [^{125}I]-Tyr-acein ([^{125}I]-JMV3042) as tracer ligand and were carried out: (A) on CHO-ACE cell membranes, data are representative of three separate experiments, each performed in duplicate, and (B) on striatal membranes, data are means of five separate experiments, each performed in duplicate. All K_i constants were determined using GraphPad PRISM v6 software.

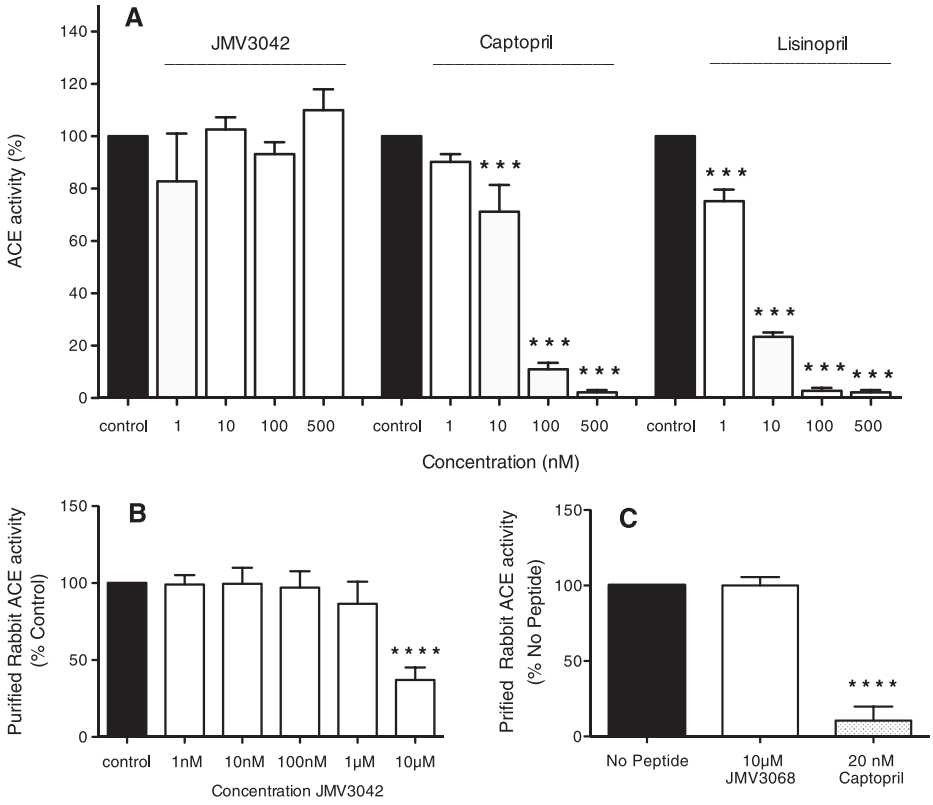


Figure 7

ACE peptidase activity. (A) Effect of H-Tyr-acein (JMV3042), captopril and lisinopril, on ACE peptidase activity on CHO-ACE cell membranes. The histogram depicts the mean (±SD) relative activity of ACE expressed in percent of control ACE peptidase activity, obtained in the absence of JMV3042. Data are representative of five separate experiments performed in duplicate. ***$P < 0.001$, significant effect of captopril or lisinopril; one-way ANOVA, Newman–Keuls *post hoc* test. (B) Effect of different concentrations of H-Tyr-acein (JMV3042) on ACE peptidase activity of rabbit lung ACE. The histogram depicts the mean (±SD) relative activity of ACE expressed in percent of control ACE activity. Data are representative of six separate experiments performed in duplicate. ****$P < 0.0001$, compared with all other treatments; Newman–Keuls *post hoc* analysis. (C) Effect of JMV3068 and captopril on ACE peptidase activity of rabbit lung ACE. The histogram depicts the mean (±SD) relative activity of ACE expressed in percent of control ACE activity. Data are representative of five separate experiments performed in duplicate. ****$P < 0.0001$, compared with all other treatments; Newman–Keuls *post hoc* analysis.

activities through its peptidase activity. In addition to the classical circulating humoral renin-angiotensin system (RAS), in which ACE plays a central role, there exists a second RAS or local/tissue RAS in many tissues, including brain tissue (Re, 2004) that contains the different components of the circulating RAS (von Bohlen und Halbach and Albrecht, 2006), with no particular activity, unrelated to its peptidase activity described so far. Although the precise role of brain RAS remains unclear, a number of recent reviews have highlighted its significance in age-related neurodegenerative changes (Savaskan, 2011; Saavedra, 2012; Ohshima *et al.*, 2013; Naffah-Mazzacoratti *et al.*, 2014).

Among the components of the brain RAS, ACE has been identified as a key player, having an increased activity in ageing, resulting in neurodegeneration, which induces learning, memory impairments and dementia. Besides, several studies have demonstrated relationships between RAS, angiotensin derivatives and dopamine (Labandeira-Garcia *et al.*, 2014), which are critical for movement, motivation and cognition (Rice *et al.*, 2011).

Some studies indicate that angiotensin II stimulates *in vitro* and *in vivo* the release of dopamine in the striatum of rats (Simonnet and Giorguieff-Chesselet, 1979; Mendelshon *et al.*, 1993). For instance, angiotensin II induces turning behaviour in 6-hydroxydopamine lesioned rats, while no effect on normal rats was observed. This effect was blocked by the AT_1 receptor antagonist losartan, suggesting that dopamine release was mediated by AT_1 receptors (Jenkins *et al.*, 1995). Using ACE inhibitors, some authors have shown that ACE might be indirectly involved in modulation of dopamine release. In one study, a single dose of the ACE inhibitor ceranapril (10 $\mu g \cdot kg^{-1}$, i.p.) increased dopamine release in the amygdala, with no significant changes in the striatum (Barnes *et al.*, 1992). In another study, treatment (1 week p.o.) with 1 $mg \cdot kg^{-1} \cdot day^{-1}$ perindopril, an ACE inhibitor shown to cross the blood brain barrier, induced a nearly 2.5 times increase in striatal dopamine levels (Jenkins *et al.*, 1997, Jenkins, 1998). Also, captopril (10 µM) significantly inhibited stimulation-evoked [^{3}H]-dopamine release from rat striatal slices, in a concentration-dependent manner,

while the basal release of [^{3}H]-dopamine was not affected (Tsuda *et al.*, 1998). In our study, we showed that H-Tyr-acein did not recognize the AT1 receptor. Taken together, these results show that relations between ACE, its products including mainly angiotensin II, and dopamine release are still not clearly understood.

Deregulation of dopaminergic transmission is known to be involved in a wide number of pathologies including Parkinson's disease (PD) (Labandeira-Garcia *et al.*, 2012), in which evidence for RAS involvement has been accumulating over the last decade (Mertens *et al.*, 2010). Because the dopamine precursor L-DOPA, although not fully satisfactory, is currently one of the most effective treatments for the relief of the motor symptoms of the disease, any therapeutic approach targeting stimulation of dopamine release for treatment of PD could constitute a promising alternative.

The potential of the brain RAS as a target for Alzheimer's disease (AD) comes from the observation of its effects on learning and memory (Gard, 2004). In support of these findings, ACE inhibitors and angiotensin analogues enhanced cognitive processing, being effective in delaying or reversing symptoms of AD or PD in both human and animal models (Ohrui *et al.*, 2004; Kehoe and Wilcock, 2007; Yamada *et al.*, 2011). On the other hand, some studies have indicated that ACE significantly inhibited the aggregation, deposition and cytotoxicity of amyloid β peptide *in vitro*, by degrading amyloid β(1–40) (Hu *et al.*, 2001).

Based on the results concerning the relationships between angiotensin II, its derivatives, ACE inhibitors and dopamine release (Wright and Harding, 2004) (Labandeira-Garcia *et al.*, 2014), angiotensin II, its derivatives and ACE inhibitors have been evaluated in neurological disorders, including PD and AD. However, although the different studies have pointed out the significance of RAS in the brain, its precise role is still unclear, and the protective effects of ACE products and ACE inhibitors in neurodegenerative diseases, particularly in PD and AD, remains largely misunderstood (Soto et al., 2013; Wright *et al.*, 2013).

In conclusion, this study shows that acein, a synthetic peptide with specific structural characteristics, interacts with high affinity with brain membrane-bound ACE of rodents, at a different site from the active site involved in the well-known peptidase activity.

Acein was able to induce *in vivo* and *in vitro* stimulation of dopamine release from rat brain tissue. While the mechanism of action of acein is still unknown, this presynaptic stimulation of dopamine release could be direct or indirect, through other striatal neurotransmitters. Accordingly, although far from being fully demonstrated, it is a possibility that ACE not only possesses an enzymic peptidase activity but that it might also be associated with stimulation of dopamine release, exhibiting a receptor-like biological activity, in addition to its well-known peptidase activity. In this case, brain ACE could provide a new target for ligands that might interact with the mechanisms underlying brain diseases, particularly those in which dopamine is involved. Acein would be the first described candidate able to interact with this target. These results might suggest a more important role for brain ACE than initially described.

Additionally, considering interactions between the RAS and the dopaminergic system, the role of acein has also to be investigated in the peripheral system, in particular with regard to the regulation of renal sodium excretion and cardiovascular functions.

Acknowledgements

We thank P Corvol and A Michaud (Collège de France, Paris) for providing CHO-ACE cells, C Rouch and S Perez for technical assistance and M Séveno in charge of the proteomic platform, the 'Laboratoires Ipsen-Beaufour', Les Ulis, France, for their support in the studies concerning the search for amidated peptides and for the discussions with PJ Moreau, E Ferrandis, JA Camara and CA Thurieau. We are particularly indebted to P Wender, Stanford University, USA, for his fruitful discussions, suggestions and remarks; P Corvol and C Llorens-Cortes, Collège de France, Paris, France; and M Morris, IBMM, Montpellier, France, for helpful discussions. We thank J Miller for reading the manuscript for the English style. J Neasta was supported by a CNRS Postdoctoral Fellowship.

Author contributions

K.P., J.N., J-L.B., J.Marie, J-C.G., D.G., E.C., C.M. and N.B. were involved in performing *in vitro* pharmacology; V.D. and A-C.C. performed *in vivo* experiments; M-L.K. carried out *in vitro* experiments related to dopamine release; C.V. and G. S. were involved in the synthesis of compounds and S.C., Ph.M., in MS and proteomics experiments and analyses; G. B. wrote the bioinformatics programme; J.N., J-L.B., J.Marie, K.P., V.D. and J. Martinez, analysed the data; J. Martinez initiated and managed the project, wrote the paper with the help of other co-authors and is the corresponding author of this study. All authors read and approved the final paper.

Conflict of interest

The authors declare no conflicts of interest.

Declaration of transparency and scientific rigour

This Declaration acknowledges that this paper adheres to the principles for transparent reporting and scientific rigour of preclinical research recommended by funding agencies, publishers and other organisations engaged with supporting research.

References

Alexander SPH, Fabbro D, Kelly E, Marrion N, Peters JA, Benson HE, *et al.* (2015a). The Concise Guide to PHARMACOLOGY 2015/16: Enzymes. Br J Pharmacol 172: 6024–6109.

Alexander SPH, Davenport AP, Kelly E, Marrion N, Peters JA, Benson HE, *et al.* (2015b). The Concise Guide to PHARMACOLOGY 2015/16: G Protein-Coupled Receptors. Br J Pharmacol 172: 5744–5869.

Amare A, Hummon AB, Southey BR, Zimmerman TA, Rodriguez-Zas SL, Sweedler JV (2006). Bridging neuropeptidomics and genomics

with bioinformatics: prediction of mammalian neuropeptide prohormone processing. J Proteome Res 5: 1162–1167.

Barnes JM, Barnes NM, Costall B, Coughlan J, Kelly ME, Naylor RJ, *et al.* (1992). Angiotensin-converting enzyme inhibition, angiotensin, and cognition. J Cardiovasc Pharmacol 19: S63–S71.

Berendse HW, Galis-de-Graaf Y, Groenewegen HJ (1992). Topographical organization and relationship with ventral striatal compartments of prefrontal corticostriatal projections in the rat. J Comp Neurol 316: 314–347.

Bernstein KE, Ong FS, Blackwell WL, Shah KH, Giani JF, Gonzalez-Villalobos RA, *et al.* (2013). A modern understanding of the traditional and non-traditional biological functions of angiotensin-converting enzyme. Pharmacol Rev 65: 1–46.

Camara Y, Ferrer JA, Thurieau CA, Martinez J, Berge G, Goze C, Giani JF, Gonzalez-Villalobos RA, *et al.* (2000). Rational selection of putative peptides from identified nucleotide, or peptide sequences, of unknown function. *Patent* PCT WO 2000/50636.

Carmona AK, Schwager SL, Juliano MA, Juliano L, Sturrock ED (2006). A continuous fluorescence resonance energy transfer angiotensin I-converting enzyme assay. Nature Protocol. 1: 1971–1976.

Chan WC, White PD (2000). Fmoc solid phase peptide synthesis: a practical approach. In: Hammes BD (ed). The Practical Approach Series. Oxford University Press: Oxford.

Curtis MJ, Bond RA, Spina D, Ahluwalia A, Alexander SPH, Giembycz MA, *et al.* (2015). Experimental design and analysis and their reporting: new guidance for publication in *BJP*. Br J Pharmacol 172: 3461–3471.

Gard PR (2004). Angiotensin as a target for the treatment of Alzheimer's disease, anxiety and depression. Exp Opin Ther Targets 8: 7–14.

Gras C, Amilhon B, Lepicard EM, Poirel O, Vinatier J, Herbin M, *et al.* (2008). The vesicular glutamate transporter VGLUT3 synergizes striatal acetylcholine tone. Nat Neurosci 11: 292–300.

Greenwood FC, Hunter WM, Glover JS (1963). Preparation of ^{131}I-labelled human growth hormone of high specific radioactivity. Biochem J 89: 114–123.

Hinuma S, Shintani Y, Fukusumi S, Iijima N, Matsumoto Y, Hosoya M, *et al.* (2000). New neuropeptides containing carboxy-terminal RFamide and their receptor in mammals. Nat Cell Biol 2: 703–708.

Hu J, Igarashi A, Kamata M, Nakagawa H (2001). Angiotensin-converting enzyme degrades Alzheimer amyloid beta-peptide (Ab) retards A-beta aggregation, deposition, fibril formation; and inhibits cytotoxicity. J Biol Chem 276: 47863–47868.

Hummon AB, Richmond TA, Verleyen P, Baggerman G, Huybrechts J, Ewing MA, *et al.* (2006). From the genome to the proteome: uncovering peptides in the Apis brain. Science 314: 647–649.

Jenkins TA (1998). Effects of angiotensin-related antihypertensives on brain neurotransmitter levels in the rats. Neurosci Letters 444: 186–189.

Jenkins TA, Chai SY, Howells DW, Mendelsohn FAO (1995). Intrastriatal angiotensin II induces turning behaviour in 6-hydroxydopamine lesioned rats. Brain Res 691: 213–216.

Jenkins TA, Mendelsohn FAO, Chai SY (1997). Angiotensin-converting enzyme modulates dopamine turnover in the striatum. J Neurochem 68: 1304–1311.

Kehoe PG, Wilcock GK (2007). Is inhibition of the renin-angiotensin system a new treatment option for Alzheimer's disease. Lancet Neurol 6: 373–378.

Kilkenny C, Browne W, Cuthill IC, Emerson M, Altman DG (2010). NC3Rs Reporting Guidelines Working Group. Br J Pharmacol 160: 1577–1579.

Kojima M, Hosoda H, Date Y, Nakazato M, Matsuo H, Kangawa K (1999). Ghrelin is a growth-hormone-releasing acylated peptide from stomach. Nature 402: 656–660.

Krebs MO, Trovero F, Desban M, Gauchy C, Glowinsky J, Kemel ML (2002). Distinct presynaptic regulation of dopamine release through NMDA receptors in striosome-enriched and matrix-enriched areas of the rat striatum. J Neurosci 11: 1256–1262.

Labandeira-Garcia JL, Rodriguez-Pallares J, Rodriguez-Perez AI, Garrido-Gil P, Villar-Cheda B, Valezuela R, *et al.* (2012). Brain angiotensin and dopaminergic degeneration: relevance to Parkinson's disease. Am J Neurodegenerative Dis 1: 226–244.

Labandeira-Garcia JL, Garrido-Gil P, Rodriguez-Pallares J, Valezuela R, Borrajo A, Rodriguez-Perez AI, *et al.* (2014). Brain renin–angiotensin system and dopaminergic cell vulnerability. Frontiers in Neuroanatomy 8: 1–8.

Ladurelle N, Roques BP, Dauge V (1995). The transfer of rats from a familiar to a novel environment prolongs the increase of intracellular dopamine efflux induced by CCK8 in the posterior nucleus-accumbens. J Neurosci 15: 3118–3127.

Ladurelle N, *et al* (1997). The CCK-B agonist, BC264, increases dopamine in the nucleusaccumbens and facilitates motivation and attention after intraperitoneal injection in rats. Eur J Neurosci 9: 1804–1814.

Leyris JP, Roux T, Trinquet E, Verdie P, Fehrentz JA, Oueslati N, *et al.* (2011). Homogeneous time-resolved fluorescence-based assay to screen for ligands targeting the growth hormone secretagogue receptor type 1a. Anal Biochem 408: 253–262.

Martinez J, Goze C (1999). Probes and primers for identifying nucleic acids encoding precursors of amidated polypeptide hormones. *Patent* PCT WO 99/10361.

Mazurski EJ, Beninger RJ (1991). Effects of selective drugs for dopaminergic D1 and D2 receptors on conditioned locomotion in rats. Psychopharmacol 105: 107–112.

McGeorge AJ, Faull RLM (1989). The organization of the projection from the cerebral cortex to the striatum in the rat. Neurosci 29: 503–537.

McGrath JC, Lilley E (2015). Implementing guidelines on reporting research using animals (ARRIVE etc.): new requirements for publication in BJP. Br J Pharmacol 172: 3189–3193.

Mendelsohn FAO, Jenkins TA, Berkovic SF (1993). Effects of angiotensin-II on dopamine and serotonin turnover in the striatum of conscious rats. Brain Res 613: 221–229.

Mendre C, Rodriguez M, Gueudet C, Lignon MF, Galas MC, Laur J, *et al.* (1988). A pseudopeptide that is a selective central cholecystokinin receptor antagonist. J Biol Chem 263: 10641–10645.

Mertens B, Vanderheyden P, Michotte Y, Sarre S (2010). The role of the central renin–angiotensin system in Parkinson's disease. J Renin-Angiotensin-Aldosterone System 11: 49–56.

Mirabeau O, Perlas E, Severini C, Audero E, Gascuel O, Possenti R, *et al.* (2007). Identification of novel peptide hormones in the human proteome by hidden Markov model screening. Genome Res 17: 320–327.

Mousseaux D, Le Gallic L, Ryan J, Oiry C, Gagne D, Fehrentz JA, *et al.* (2006). Regulation of ERKI/2 activity by ghrelin-activated growth hormone secretagogue receptor 1A involves a PLC/PKC epsilon pathway. Br J Pharmacol 148: 350–365.

Naffah-Mazzacoratti MG, Gouvela TL, Simoes PS, Perosa SR, *et al.* (2014). What have we learned about the kallikrein–kinin and renin–angiotensin systems in neurological disorders? World J Biol Chem 5: 130–140.

Ohshima K, Mogi M, Horiuchi M (2013). Therapeutic approach for neuronal disease by regulating renin–angiotensin system. Current Hypertension Rev 9: 99–107.

Ohrui T, Tomita N, Sato-Nakagawa T, Matsui T, Maruyama M, Niwa K, *et al.* (2004). Effects of brain-penetrating ACE inhibitors on Alzheimer disease progression. Neurology 63: 1324–1335.

Olsen JV, de Godoy LM, Li G, Macek B, Mortensen P, Pesch R, *et al.* (2005). Parts per million mass accuracy on an orbitrap mass spectrometer via lock mass injection into a C-trap. Mol Cell Proteomics 4: 2010–2021.

Pawson AJ, Sharman JL, Benson HE, Faccenda E, Alexander SPH, Buneman OP, et al. , NC-IUPHAR(2014). The IUPHAR/BPS Guide to PHARMACOLOGY: an expert-driven knowledge base of drug targets and their ligands. Nucl Acids Res 42 (Database Issue): D1098–D1106.

Paxinos G, Watson C (2007). The rat brain in stereotaxic coordinates, Sixth edition, Academic Press.

Re RN (2004). Tissue renin angiotensin systems. Med Clin North Am 88: 19–38.

Rice ME, Patel JC, Cragg SJ (2011). Dopamine release in the basal ganglia. Neuroscience 198: 112–137.

Saavedra JM (2012). Angiotensin II AT(1) receptor blockers ameliorate inflammatory stress: a beneficial effect for the treatment of brain disorders. Cell Mol Neurobiol 32: 667–681.

Savaskan E (2011). The renin–angiotensin system in neurodegenerative diseases. Schweizer Archiv Für Neurologie Und Psychiatrie 162: 119–121.

Sebret A, Lena I, Crete D, Matsui T, Roques BP, Dauge V (1999). Rat hippocampal neurons are critically involved in physiological improvement of memory processes induced by cholecystokinin-B receptor stimulation. J Neurosci 19: 7230–7237.

Shenone M, Dancik V, Wagner BK, Clemons PA (2013). Target identification and mechanism of action in chemical biology and drug discovery. Nat Chem Biol 9: 232–240.

Simonnet G, Giorguieff-Chesselet MF (1979). Stimulating effect of angiotensin-II on the spontaneous release of newly synthesised [^{3}H] dopamine in rat striatal slices. Neurosci Letters 15: 153–158.

Sonsalla PK, Coleman C, Wong LY, Harris SL, Richardson JR, Gadad BS, Li W, German DC (2013). The angiotensin converting enzyme inhibitor captopril protects nigrostriatal dopamine neurons in animal models of parkinsonism. Exp Neurol 250: 376–83.

Soto M, van Kan GA, Nourhashemi F, Gillette-Guyonnet S, Cesari M, Cantet C, *et al.* (2013). Angiotensin-converting enzyme inhibitors and Alzheimer's disease progression in older adults: results from the réseau sur la maladie d'Alzheimer français cohort. J Am Geriatr Soc 61: 1482–1488.

Strittmatter SM, Lo MM, Javitch JA, Snyder SH (1984). Autoradiographic visualization of angiotensin-converting enzyme in rat-brain with [^{3}H]captopril: localization to a striatonigral pathway. Proc Natl Acad Sci U S A 81: 1599–1603.

Tsuda K, Tsuda S, Nishio I, Masuyama Y, Goldstein M (1998). Captopril inhibits both dopaminergic and cholinergic neurotransmission in the central nervous system. Clin Exp Pharmacol Physiol 25: 904–907.

von Bohlen und Halbach O, Albrecht D (2006). The CNS renin–angiotensin system. Cell Tissue Res 326: 599–616.

Wei L, Alhenc-Gelas F, Soubrier F, Michaud A, Corvol P, Clauser E (1991). Expression and characterization of recombinant angiotensin I-converting enzyme – evidence for a C-terminal membrane anchor and for a proteolytic processing of the secreted recombinant and plasma enzymes. J Biol Chem 266: 5540–5546.

Wilm M, Shevchenko AJ, Houthaeve T, Breit S, Schweigerer L, Fotsis L, *et al.* (1996). Femtomole sequencing of proteins from polyacrylamide gels by nano-electrospray mass spectrometry. Nature 379: 466–469.

Wright JW, Harding JW (2004). The brain angiotensin system and extracellular matrix molecules in neural plasticity, learning, and memory. Prog Neurobiol 72: 263–293.

Wright JW, Kawas LH, Harding JW (2013). A role for the brain RAS in Alzheimer's and Parkinson's diseases. Frontiers in Endocrinol 4: 1–12.

Yamada K, Horita T, Takayama M, Takahashi S, Takaba K, Nagata Y, *et al.* (2011). Effect of centrally active angiotensin-converting enzyme inhibitor, perindopril, on cognitive performance in chronic cerebral hypo-perfusion rats. Brain Res 1421: 110–120.

Zhuo J, Moeller I, Jenkins T, Chai SY, Allen AM, Ohishi M, *et al.* (1998). Mapping tissue angiotensin-converting enzyme and angiotensin AT_1, AT_2 and AT_4 receptors. J Hypert 16: 2027–2037.

Supporting Information

Additional Supporting Information may be found in the online version of this article at the publisher's web-site:

http://dx.doi.org/10.1111/bph.13424

Figure S1 Acein-induced contralateral rotations of rat, after 0.5 and 5 fmol acein (JMV3041) injection in the sensorimotor territory of the dorsal striatum. (n = 10) [$F_{(2,28)}$ = 15.611, $P <$ 0.001]. ***$P < 0.001$ vs control, Dunnett's test.

Figure S2 Mass spectrometry identification of ACE as the striatal protein target of acein. (A) 40 μg of guinea pig striatal membrane proteins were incubated with 50 nM of Biot-Ahx-Tyr-Bpa-Pro-Pro-Thr-Thr-Thr-Lys-Phe-Ala-Ala-OH (JMV5394) in the absence or in the presence of 5 μM of H-Tyr-acein (JMV3042) and then UV-irradiated. The resulting biotinylated proteins were analysed by SDS-PAGE followed by streptavidin overlay to detect biotinylated proteins (n = 3). (B) 800 μg of striatal membrane proteins were UV crosslinked to JMV5394, pulled-down with streptavidin and proteins were revealed with silver staining following SDS-PAGE (n = 3). (C) Two gel slices corresponding to the specific band were cut out in control (C) and test (T) lanes and proteins were in-gel digested with trypsin. The resulting peptides were submitted to MS/MS analysis for protein identification. Figure S2C shows the six top hits resulting from MS/MS protein identification and the number of unique peptides that led to these identifications. The complete list of proteins that were identified MS is provided in/MS is provided in Table S2A of Supporting Information. (D) H0UWL7_CAVPO amino acid sequence was blasted against UniProtKB/Swiss-Prot protein database using protein-protein blast algorithm (Blast-p). The Table shows the five top hits resulting from this interrogation.

Figure S3 Validation of ACE as the target of acein. (A) 400 μg of guinea pig striatal membrane proteins were incubated with 50 nM of Biot-Ahx-Tyr-Bpa-Pro-Pro-Thr-Thr-Thr-Lys-Phe-Ala-Ala-OH (JMV5394) in the absence or in the presence of 5 μM of H-Tyr-acein (JMV3042) and UV-irradiated. The resulting biotinylated proteins were pulled-down with

agarose resin coupled to streptavidin and the presence of ACE proteins was examined by Western blot analysis using an anti-ACE antibody ($n = 2$). (B) 4 μg of purified rabbit lung ACE were incubated with 50 nM of JMV5394 either in the presence of 1 μM of H-Tyr-acein or in the presence of 1 μM of ghrelin, followed by UV irradiation. 15 % of the resulting protein mixture was resolved by SDS-PAGE, transferred to nitrocellulose membrane and immunoblotted with the anti-ACE antibody (top panel). Then, the formation of the JMV5394-ACE complex was examined by streptavidin overlay on the same nitrocellulose membrane (lower panel) ($n = 3$).

Figure S4 Characterisation of the binding properties of [^{125}I]-Tyr-acein ([^{125}I]-JMV3042) on CHO-ACE cell membranes. Saturation experiments were performed on CHO-ACE cell membranes. Non-specific binding was determined by adding a final concentration of 10 μM unlabelled H-Tyr-acein. Kd and Bmax values were determined by non-linear regression analysis of saturation binding data using GraphPad PRISM v6 software. Reported values are means of 3 separate experiments, each performed in duplicate.

Figure S5 Binding properties of acein analogues to CHO-ACE cell membranes. Competition curves were obtained with 0.5 nM [^{125}I]-Tyr-acein ([^{125}I]-JMV3042) as tracer ligand. Ki constants were determined using GraphPad PRISM v6 software. Data are means of 3 separate experiments, each performed in duplicate.

Table S1 Compounds tested for their ability to displace [^{125}I]-Tyr-acein ([^{125}I]-JMV3042) from its binding sites on whole guinea pig brain membranes. None of the tested compounds at 1 μM concentration was able to significantly displace labelled acein from its binding sites.

Table S2 Summary of MS/MS data that led to the identification of H0UWL7_CAVPO protein as the striatal target of acein. (A), Complete list of proteins identified by MS/MS analysis in the test gel slice (T) and in the corresponding control gel slice (see also Figures S2C, S2D). The percent amino acid coverage for each protein and the number of unique peptides identified in each gel slice are also listed. (B) List of tryptic peptides that led to H0UWL7_CAVPO protein identification by MS/MS analysis.